Published in final edited form as:
Invest Ophthalmol Vis Sci. 2008 June ; 49(6): 2303–2314.

Factors Affecting Perceptual Thresholds in Epiretinal Prostheses

Chloé de Balthasar[1], **Sweta Patel**[1], **Arup Roy**[2], **Ricardo Freda**[1,3], **Scott Greenwald**[2], **Alan Horsager**[1], **Manjunatha Mahadevappa**[1,3], **Douglas Yanai**[1,3], **Matthew J. McMahon**[2], **Mark S. Humayun**[1,3], **Robert J. Greenberg**[2], **James D. Weiland**[1,3], and **Ione Fine**[1,4]

1*Department of Ophthalmology and Zilkha Neurogenetic Institute, University of Southern California, Los Angeles, California*

2*Second Sight Medical Products, Inc., Sylmar, California*

3*Doheny Eye Institute, Los Angeles, California*

4*Department of Psychology, University of Washington, Seattle, Washington*

Abstract

Purpose—The goal was to evaluate how perceptual thresholds are related to electrode impedance, electrode size, the distance of electrodes from the retinal surface, and retinal thickness in six subjects blind as a result of retinitis pigmentosa, who received epiretinal prostheses implanted monocularly as part of a U.S. Food and Drug Administration (FDA)–approved clinical trial.

Methods—The implant consisted of an extraocular unit containing electronics for wireless data, power recovery, and generation of stimulus current, and an intraocular unit containing 16 platinum stimulating electrodes (260- or 520-μm diameter) arranged in a 4 × 4 pattern. The electrode array was held onto the retina by a small tack. Stimulation was controlled by a computer-based external system that allowed independent control over each electrode. Perceptual thresholds (the current necessary to see a percept on 79% of trials) and impedance were measured for each electrode on a biweekly basis. The distance of electrodes from the retinal surface and retinal thickness were measured by optical coherence tomography on a less regular basis.

Results—Stimulation thresholds for detecting phosphenes correlated with the distance of the electrodes from the retinal surface, but not with electrode size, electrode impedance, or retinal thickness.

Conclusions—Maintaining close proximity between the electrode array and the retinal surface is critical in developing a successful retinal implant. With the development of chronic electrode arrays that are stable and flush on the retinal surface, it is likely that the influence of other factors such as electrode size, retinal degeneration, and subject age will become more apparent.

Corresponding author: Ione Fine, Department of Psychology, Guthrie Hall, Room 233, Box 351525, University of Washington, Seattle, WA 98195; ionefine@u.washington.edu..

Disclosure: **C. de Balthasar**, None; **S. Patel**, Second Sight Medical Products, Inc. (E); **A. Roy**, Second Sight Medical Products, Inc. (E, P); **R. Freda**, None; **S. Greenwald**, Second Sight Medical Products, Inc. (E); **A. Horsager**, None; **M. Mahadevappa**, None; **D. Yanai**, None; **M.J. McMahon**, Second Sight Medical Products, Inc. (E, P); **M.S. Humayun**, Second Sight Medical Products, Inc. (F); **R.J. Greenberg**, Second Sight Medical Products, Inc. (E); **J.D. Weiland**, Second Sight Medical Products, Inc. (F); **I. Fine**, Second Sight Medical Products, Inc. (C, P, R)

Photoreceptor loss in diseases such as retinitis pigmentosa (RP) and age-related macular degeneration (AMD) are two of the leading causes of blindness.[1–3] In recent years, several research groups have had the goal of developing an electronic retinal prosthesis to restore some vision within individuals with these diseases.[4–8]

A major concern in the field has been that the charge density needed to elicit light percepts may be too high to permit long-term stimulation without causing damage to the retina. A second concern is that the current amplitude necessary to elicit percepts may fluctuate unpredictably over time, due to neurophysiological changes in the wiring of the retina, damage to the retina, electrochemical changes on the electrode surface, or instability of position of the electrode array on the retinal surface. In acute studies (lasting <3 hours), it has been found that localized retinal electrical stimulation of blind subjects resulted in discrete visual percepts; however, the amount of electrical current needed to elicit visual responses was relatively large compared with that used in animal in vitro retinal studies examining responses to electrical stimulation.[9,10] A likely explanation for these high thresholds is that in acute operating room conditions, it is difficult for subjects to maintain high levels of concentration, it is difficult to control electrode distance from the retinal surface, and it is possible to perform only a very small number of trials. An alternative possibility is that the high electrical thresholds found in previous human trials were due to the effects of retinal degeneration, which include both loss of cell function and rewiring of the retina.[11–14]

We report data from six subjects implanted with epiretinal prostheses for a prolonged period. In these subjects, we repeatedly measured (over a period of several months) perceptual thresholds, electrode impedance, the distance of electrodes from the retinal surface, and retinal thickness. A subset of data from three subjects have been reported elsewhere.[15] Our goal was to evaluate how perceptual thresholds are related to electrode impedance, the distance of the electrodes from the retinal surface, and retinal thickness.

It has been shown[16,17] that the log threshold current necessary to elicit spikes within in vitro retinal ganglion cells correlates linearly with log electrode area. However, the relationship between electrode size and threshold is less clear in human studies. (Hornig R et al. *IOVS* 2006;47:ARVO E-Abstract 3216).[5,9,10,15] In the few studies in which data have been collected over a prolonged period, reported thresholds were based on a small number of trials, and different electrodes sizes were implanted across subjects, thereby confounding electrode array position, intersubject variability, and electrode size.[9,15]

OCT cross-sectional images of retinal tissue across multiple-depth planes, resolved to the scale of ≤10 μm, are inferred from the profile of near-infrared backscattered light. OCT is well validated for measuring retinal thickness. However, OCT has not yet been used for measuring retinal thickness or the distance of electrodes from the retinal surface in patients with implanted retinal prostheses.

The distance of electrodes from the retinal surface is likely to be a critical factor in determining the amount of current necessary to produce a percept. Both modeling and animal electrophysiology data suggest that electric current diminishes with the distance from the electrode in retinal stimulation.[18,19] An additional concern is that current injected from electrodes that are distant from the retina will affect a larger area on the retina, thus decreasing the spatial resolution of the stimulation.[19,20]

Retinal thickness is associated with the extent of retinal degeneration,[21] and it is possible that the ability to elicit percepts through electrical stimulation is compromised in patients in advanced stages of RP. Although bipolar, amacrine, and ganglion cells are still present in later stages of these diseases, their numbers are significantly decreased,[11,14,22] and their spatial organization and circuitry are severely disorganized.[12]

We were also interested in determining whether, in retinal implants, impedance might provide a potential means of assessing the distance of the electrodes from the retina, changes to retinal tissue local to the implant, or the perceptual threshold for electrical stimulation. Electrode impedance provides a measure of electrical resistance to current that is determined primarily by electrode material, electrode size, and the tissue surrounding the electrode. Impedance has been successfully used in cochlear implants to assess the positional stability of the implant, the electrochemical and electronic integrity of the implant, and the neurophysiological status of the surrounding tissue. In the early weeks after implantation, changes in impedance in cochlear implants have been associated with inflammatory tissue responses, the growth of fibrous or scar tissue,[23] and the formation of a hydride layer on the surface of the electrode.[24,25] After an initial period of instability, impedances can remain stable for several years.[26,27] In cochlear implants, these stable impedances do not seem to correlate particularly well with the distance of the electrode from the modiolar wall.[28]

Materials and Methods

Subject Selection, Implantation, and Testing History

The study protocol was granted an Investigational Device Exemption (IDE) by the U.S. Food and Drug Administration (FDA), was approved by the Institutional Review Board at the University of Southern California and adhered to the tenets of the Declaration of Helsinki. Six subjects (S) with severe RP participated in the study. Four (S2–S5) had scant light perception only in the worse eye, and two (S1 and S6) had no light perception (NLP) in the worse eye. A series of standard and specialized preoperative tests were used to confirm each subject's visual acuity and to assess general ophthalmic health. This preoperative evaluation included a complete eye examination, electroretinogram, visual evoked potential, bright flash detection, electrically evoked responses, fluorescein angiography, and fundus photography.[29]

Table 1 includes the subjects' ages at the date of implantation, preoperative acuity, the number of days over which we collected data for each subject, electrode sizes implanted in each subject, and eye of implantation. In subjects with a difference in preoperative vision between the two eyes, implantation was performed in the eye with the worse vision. One subject (S2) underwent surgery twice in the same eye because her electrode array detached from the retina after 11 months due to falling and bumping her head (no retinal detachment occurred). In the second surgery, the electrode array was reattached in a nearby macular area no more than 500 μm distant from the position of the original implant. Testing of S1 was limited in duration because of geographical constraints. Testing of S3 ended for medical reasons unrelated to the implant. Testing of S4 was ended after microperforation of her conjunctiva, which led to exposure of the cable. Because her cardiac status had deteriorated since the initial implantation, she could not undergo anesthesia and, therefore, could not undergo the use of a scleral patch graft to repair the microperforation. The risk of infection was minimized by cutting the multiwire cable connecting the electrode array to the extraocular stimulator, and the electrode array was left in place. Testing of S2, S5, and S6 was ongoing as of March 15, 2007.

Testing sessions lasted a maximum of 4 hours, with frequent rest periods. The sessions included threshold and impedance measurements, as well as other measures of visual performance reported elsewhere.[7] When performed, threshold measurements were usually obtained at the beginning of a given testing session. The frequency of testing sessions was limited by the subjects' availability and the clinical trial protocol. In general, each subject took part in one to two sessions per week. Our protocol specified that OCT measurements were performed on the subjects only for clinical reasons, and as a result OCT data were collected at irregular intervals.

Intraocular and Extraocular Component Configuration

Figure 1 shows a fundus image of the intraocular electrode array in S3 viewed through a dilated pupil. As described previously,[30] the array consisted of 16 platinum electrodes in a 4 × 4 arrangement, held in place within a clear silicone rubber platform. The array was attached to the retina using a retinal tack. The electrode diameters were 520 μm (corresponding to 1.8° of visual angle) in S1 and S2, 260 μm (0.9° of visual angle) in S3, and a checkerboard arrangement with alternating 260- and 520-μm electrodes was used in S4, S5, and S6 (Table 1, Fig. 2a). In all subjects, the center-to-center separation between electrodes was 800 μm. The distant return electrode was placed on the electronics case, and a 16-wire SC cable connected the intraocular electrode array to the extraocular unit through the sclera.

External Components

The extraocular component of the implant, which converts a radio frequency signal into electrical stimulation patterns, was surgically implanted in the temporal bone, similar to a cochlear implant.[31] Implant data and power were transmitted via an inductive wireless link, with an external antenna magnetically aligned over the electronic implant. The desired pulse pattern was generated on a computer and sent to a custom-built video processing unit (Second Sight Medical Products, Inc., Sylmar, CA) that coded the data as a serial data stream and transmitted it to the implant via the wireless link. A reverse telemetry function in the implant allowed direct measurement of the impedance of each electrode.[30] The subject's nonsurgical eye was patched to ensure that the thresholds were not affected by any residual vision in that eye.

Optical Coherence Tomography

Figure 2a shows a fundus image in S6 of an intraocular electrode array with the OCT imaging light source visible (a single line). The arrow represents the direction of the imaging. Figure 2b shows the image of the cross-section of the retina that lay under the OCT imaging light source in Figure 2a. Broad shadows are cast by the electrodes, and narrow shadows are due to the passage of the imaging light source across the edge of the electrode (as is the case in electrode 3 in this example) or are cast by individual wires within the array (note that wires also pass above individual electrodes). Corresponding electrodes are labeled across Figures 2a and 2b. As mentioned, the electrodes in this subject alternated between 520 and 260 μm. Electrodes 1 and 3 were 260 μm in diameter, and electrodes 2 and 4 were 520 μm in diameter. The small deviation between the position of the scan line in the fundus image and the actual OCT image position was due to the occurrence of slight eye movements in the very short time interval that separated acquisition of the two images.

Because our subjects have nystagmus (uncontrolled eye movement), obtaining clear OCT images was time consuming and physically demanding. Consequently, OCT measurements could not be gathered for every electrode for every subject. OCT data were not available for S1, because the OCT apparatus was not available when this subject was being tested.

As shown in Figure 2b, we measured the distance from the top of each electrode to the internal limiting membrane of the retina (red arrows). This measurement included the electrode thickness, which varied between 80 and 120 μm, depending on the exact cross-section of the electrode over which the OCT measurement was taken, and we therefore subtracted an estimated electrode thickness of 100 μm to obtain the electrode distance from the retina. The thickness of the retina was therefore defined as the distance from the inner surface of the retinal pigment epithelium to the internal limiting membrane (Fig. 2b, orange arrows).

As can be seen in Figure 2, it was not always easy to determine the exact position of the top of the electrode, the surface of the internal limiting membrane, or the inner surface of the retinal

pigment epithelium. Two authors (CB and SP) performed these analyses with the help of custom software (written in MatLab; The MathWorks, Natick, MA). We cross-validated their judgments by having both experimenters analyze the same subset of data. If the two experimenters' judgments correlated perfectly, then their judgments would fall along a line of slope equalling 1. The best-fitting regression for estimates of electrode distance had a slope of 1.06. A Monte-Carlo procedure in which each judgment was randomly assigned to an experimenter was used to assess whether the best-fitting regression slope for these data differed significantly from 1. Experimenters' judgments were mutually correlated ($r^2 = 0.78$; $P < 0.01$), and the regression slope did not differ significantly from 1 ($P > 0.05$, two-tailed). The best-fitting regression for estimates of retinal thickness had a slope of 0.83. Performance across observers correlated strongly ($r^2 = 0.85$; $P < 0.01$), and our Monte-Carlo procedure demonstrated that regression slope did not differ significantly from 1 ($P > 0.05$, two-tailed). The high consistency across experimenters demonstrates that trained observers could make consistent judgments about electrode distance and retinal thickness on the basis of our OCT images.

Impedance

Impedance was measured with proprietary software (Second Sight Medical Products) or with a handheld portable cochlear implant tester (PCIT; Advanced Bionics, Sylmar, CA). Impedance measurements were taken at the beginning and end of each stimulating session.

Perceptual Thresholds

Perceptual thresholds were defined as the amount of current required for a subject to detect a pulse in 79% of trials.[31] We measured detection thresholds for each of the 16 electrodes using a single standard pulse, consisting of a 0.975-ms cathodic pulse followed by a 0.975-ms anodic pulse. Cathodic and anodic pulses were separated by a 0.975-ms interpulse delay. All pulse waveforms were biphasic and charge balanced.

Until September 2003, a relatively crude technique was used to measure the perceptual threshold. In each trial, subjects were given verbal feedback that a pulse was about to be presented, the subject was stimulated and was then asked to indicate verbally whether the stimulation had caused a visible percept.[15] The subject was stimulated three times at each current intensity, and the stimulation intensity was gradually increased until the subject saw the stimulation all three times. Occasional catch (nonstimulation) trials were interspersed randomly within the stimulation trials, which confirmed that subjects' false-positive rates were less than 10%. Thresholds were calculated by pooling data across sessions and the probability of the subject's reporting a percept was plotted as a function of stimulation intensity. These data were fit with a Weibull function, and threshold was defined as the stimulation intensity at which the subject reported a percept 79% of the time.[32] After September 2003, a precise yes–no procedure was used for measuring perceptual thresholds, with half the trials being catch trials. The amplitude of the test pulse was varied by using a three-up–one-down staircase. (If the subject responded correctly three times in a row, the task was made more difficult by decreasing the current amplitude, if the subject answered incorrectly on any trial, the task was made easier by increasing the current amplitude.) Each threshold was based on approximately 100 to 125 trials, generally 50 trials are adequate to estimate threshold with reasonable accuracy.[33] We confirmed that this experimental modification produced similar threshold estimates and false-positive rates by comparing thresholds collected by using the old and the new technique on several electrodes within the same experimental session. After November 2004, this procedure was automated, and subjects indicated whether they saw a stimulus on each trial via a computer key press. We again confirmed that this experimental modification did not significantly affect threshold estimates or the probability of false positive responses.

Statistical Analysis

Changes in a given measurement over time (e.g., changes in threshold or impedance over time) were analyzed by standard linear regression. Statistically significant changes over time are reported both for each subject and across all six subjects. To quantify the relationship between threshold, impedance, electrode distance, and retinal thickness, we had to find corresponding measurements over time across these different measures. We partitioned our data into 30-day time periods. For example, a given data point comparing impedance and threshold values might represent the average across several impedance measurements and several threshold measurements, both collected within the same 30-day time period (e.g., postoperative days 50 −79 inclusive). Electrode distance from the retina and retinal thickness measurements were taken less frequently, but the same approach was still applied: Electrode distance from the retina and retinal thickness estimates were compared to impedance or threshold measurements taken within the same 30-day time window as the OCT measurement.

Results

Phosphene Appearance

Phosphene appearance near threshold was typically white or yellow, and the phosphenes were reported to be round or oval. Occasionally, subjects would report seeing a dark spot. If a dark phosphene was seen in response to stimulation with a given electrode, an increase in the stimulation current generally resulted in the subject's seeing a light spot in the same location. As stimulation current increased, the brightness of the percept then tended to increase monotonically. In all subjects, phosphenes at threshold were not uncomfortable.

Stimulation Thresholds

Mean thresholds over the entire period during which we collected data are shown for each electrode and subject in Figure 3. Mean thresholds decreased dramatically across subject implantations. Thresholds in S1 varied between 173 (most sensitive electrode) and 902 (least sensitive electrode) μA. Note that subject S1 was much older than the other subjects, had no light perception (NLP) vision for much longer than any of the other subjects, and may have had confounding retinal or optic nerve damage. Platinum has a conservative, safe, long-term (i.e., long-term stimulation using pulse trains) stimulation limit of 0.35 mC/cm^2 per pulse.[34, 35] For some electrodes in S1, charge density levels above 0.35 mC/cm^2 were necessary to obtain threshold (stimulation was always kept below 1 mC/cm^2). Thresholds in S2 were also relatively high, ranging between 121 and 404 μA. By comparison, the thresholds in S6 varied between 17 and 73 μA. These differences in threshold did not change systematically with the patient's age; level of preoperative vision, as recorded clinically or measured using the dark-adapted light flash[29]; preoperative electrically evoked responses measured with a Burian-Allen corneal electrode[29]; or implant technology. However, thresholds appeared to decrease systematically across successive surgeries, perhaps because the positioning of the electrode array was successively closer to the retinal surface on each surgery. Note that there was no noticeable difference in thresholds between 260- and 520-μm electrodes, either within or across subjects.

In S5 and S6, the maximum (across all 16 electrodes) threshold was less than 100 μA for a single biphasic 0.975-ms pulse. These thresholds are well below charge density limits of 0.35 mC/cm^2, which would permit current amplitude limits of 190.6 μA for 260-μm-diameter electrodes and current amplitude limits of 762.4 μA for 520-μm electrodes. It should also be noted that these thresholds are for a single pulse, whereas functional electrical stimulation is likely to be mediated by pulse trains, which generally require lower stimulation thresholds.

Thresholds as a Function of Electrode Size

Three subjects (S4–S6) received implants of checkerboard arrays in which electrodes of 260 and 520 μm alternated in the array (Fig. 2a). We compared mean thresholds across these two electrode sizes for these three subjects. Other data shown in this article (described later) suggest that the distance of electrodes from the retinal surface has a dramatic effect on threshold. However, the checkerboard arrangement used in these three subjects provided a means of crudely factoring out the effects of electrode distance from the retinal surface. The arrays were fairly rigid, and therefore nearby electrodes tended to have similar distances from the retinal surface. This checkerboard pattern therefore tended to minimize differences in distance from the retinal surface across the two electrodes sizes in a given subject. The mean ± SE of thresholds for 260-μm electrodes were: S4, 233 ± 20.9 μA; S5, 30.3 ± 1.7 μA; and S6, 40.9 ± 6.1 μA. The mean and SE of thresholds for 560-μm electrodes were: S4, 222.9 ± 16 μA; S5, 26.9 ± 1.3 μA; and S6, 37.8 ± 4.9 μA. Contrary to expectation, electrode size did not significantly affect current threshold (Two-factor [subject × electrode size] ANOVA; $P > 0.05$ $F = 0.367$; Fig. 4a).

As described earlier, the log threshold current necessary to elicit spikes within in vitro retinal ganglion cells correlates linearly with log electrode area.[16,17] Figure 4b shows a comparison of mean thresholds for S4 to S6 with replotted data from the meta-review figure (Fig. 11 in Ref. 17) illustrating the relationship between electrode size and threshold of Sekirnjak et al.[17] Animal data replotted from their data are restricted to in vitro retinal preparations. It is possible that a wider range of electrode sizes in our subjects with implants would make threshold differences as a function of electrode size more apparent. It is also possible, given the large electrode sizes used in this experiment, that current density had a nonuniform distribution and was concentrated at the electrode edges of the electrodes (see the Discussion section).

As described in the introduction and illustrated in Figure 4b, previous acute and chronic human studies show remarkable variability in threshold (Rizzo JF III et al. *IOVS* 2000;41:ARVO Abstract S102; Hornig R et al. *IOVS* 2006;47:ARVO E-Abstract 3216).[9,15] The thresholds reported here are those of three subjects (S4–S6) who had much lower thresholds than those reported earlier by our group (S1–S3). These latter subjects demonstrate that the current levels required to elicit percepts in humans can be of the same order of magnitude as the current levels required within in vitro experiments in which similar electrode sizes are used.[16]

Stimulation Thresholds

Subject thresholds tended to increase after surgery as shown for two of the six subjects in Figure 5 (top row). As described in the Discussion section, a possible explanation for these increases is that the electrode array may have tended to lift off the retina after surgery. In all subjects except S1, there was a significant tendency for there to be a positive correlation between threshold and time since implantation (two-tailed *t*-test, $P < 0.05$). In S1, the positive correlation fell just below significance ($P = 0.057$). While reasonably well fit by a linear regression, each subject showed an individual pattern of threshold instability over time.

For each subject, we calculated absolute differences in threshold as a function of the time between the two measurements for each electrode, using every possible time-pair (for S2, each implantation was treated separately). These absolute differences in threshold as a function of time were then fit by linear regression. We found, for every subject, that the slopes of these regressions across the 16 electrodes were significantly greater than 0 (one-tailed *t*-test, S1, S2, S4, S5, and S6: $P < 0.01$; S3: $P < 0.05$). Mean slopes of the linear regression varied between 0.02 (S5) and 1.1 (S4) across subjects, corresponding to mean changes in threshold of 2 to 110

μA over a 100-day period. Thus, much of the variation in threshold across repeated measurements was due to changes in threshold over time as opposed to measurement error.

Impedance

As would be expected, impedance varied with electrode size, as shown in Figure 6 (two-factor ANOVA with replication; $P < 0.001$, $F = 146.650$). The mean and SE of impedances of 260-μm electrodes were: S4, 25.6 ± 3 kΩ; S5, 40.8 ± 1.5 kΩ; and S6, 36.5 ± 1.8 kΩ. The mean ± SE of impedances for 520-μm electrodes were: S4, 13.6 ± 1.1 kΩ; S5, 22.2.9 ± 0.3 kΩ; and S6, 18.7 ± 0.4 kΩ.

We found that impedance varied across measurements over time, as shown for two subjects in the second row of Figure 5. On the whole, subject impedances tended to decrease over time after surgery. In each subject, we calculated the best-fitting linear regression over time across all electrodes. In all subjects except S5, there was a negative correlation between impedance and time since implantation ($P < 0.05$). In S5, this negative correlation was nonsignificant ($P = 0.122$, $t = -1.6416$). In S4, S5 and S6 a separate analysis of impedances for 260- and 520-μm electrodes again found that S4 and S6 showed a negative correlation over time for both sizes of electrode, whereas in S5, the correlation again fell below significance for both electrode sizes. Although their impedances were reasonably well fit by linear regression, each subject showed an individual pattern of impedance instability over time. As described in the Discussion section, we believe that these changes in impedance may be driven by changes in the distance of the electrode array from the retinal surface.[35]

It should be noted that we also saw an initial instability in impedances in the first weeks after implantation and stimulation (the time scale of years in Fig. 5 means that this initial instability is not apparent). In patients with cochlear implants, changes in impedance in the first weeks after implantation are generally attributed to changes in the tissue surrounding the electrode and to electrochemical changes at the electrode interface.[22–24] However, because OCT measurements were taken at relatively infrequent intervals, we cannot exclude the possibility that, for our retinal implants, these early changes in impedance were affected by slight shifts in the position of the electrode array as it settled on the retina.

Array Position and Retinal Thickness

The two bottom rows of Figure 5 show measured distances of electrodes from the retinal surface and measured retinal thicknesses. Occasionally, multiple OCT images of the same electrode were taken on the same day. In these cases, measurements of electrode distance and retinal thickness for that electrode were averaged, and standard errors were calculated. Because of the difficulty in collecting OCT measurements, only a subset of electrodes was measured on any given date. Although there were clear trends within individual subjects, no clear trend over time was visible across subjects for either electrode distance or retinal thickness.

The Relationship between Threshold, Impedance, Electrode Distance, and Retinal Thickness

Figure 7 shows the relationship between threshold, impedance, electrode distance, and retinal thickness. To find corresponding measurements, we partitioned our data into 30-day periods, as described in the Methods section. As shown in Figure 7a, across all six subjects there was a significant negative correlation ($P < 0.001$) between threshold and impedance.

This correlation could be described by a power function with an exponent (e) of −1.01 and a multiplicative scaling factor (f) of 1808. This negative correlation was significant in five of the six subjects (Table 2), although the exponent varied across subjects. The exception was S5, in whom the negative correlation was nonsignificant.

As shown in Figures 4a and 6, impedances were lower for larger electrodes, yet thresholds were unaffected by electrode size. We therefore correlated thresholds and impedance separately for 260- and 520-μm electrodes. A similar negative correlation was found between threshold and impedance for both sizes of electrodes (260-μm electrodes: $e = -0.43$, $f = 5.3$, $P < 0.001$; 520-μm electrodes: $e = -1$, $f = 7.57$, $P < 0.001$). For both sizes of electrode, this negative correlation was significant in all subjects except S5 (Table 2). As described earlier, S1 and S2 received 520-μm electrodes, S3 received 260-μm electrodes, and S4, S5, and S6 received both sizes of electrode.

As shown in Figure 7b, across subjects there was a positive correlation between log electrode distance from the retina and log threshold ($e = 0.23$, $f = 3.8$, $P < 0.001$). However, this positive correlation was only significant in one (S2) of the five subjects for which OCT data were available, and was marginally significant in a second subject (S6) (see Table 2). There was therefore a strong relationship between estimated electrode–retina distance and threshold across subjects, but this correlation was not apparent within individual subjects, perhaps because OCT measurements were made infrequently and were likely to be relatively noisy.

As described in the introduction, electric fields diminish with the distance from the electrode.[18,19,36] The dependence of threshold on distance can be described by a power function for electrode–retina distances much larger than the cell body. This relationship is affected by electrode size, with larger electrodes showing a shallower increase in the amount of necessary current as a function of distance. The solid lines in Figure 7b show predicted thresholds based on a model of Palanker et al.,[19] in which the necessary voltage decrease was allowed to vary as a free parameter. The good fit of this model suggests that, for our array configuration, modeling the electric field current in an isotropic medium with distant boundaries may provide a reasonable model for electrical stimulation thresholds.

As shown in Figure 7c, across subjects there was a negative correlation between log impedance and log distance of the electrode from the retinal surface ($e = -0.08$, $f = 3.08$, $P < 0.01$). However, the exponent was significantly less than 0 in only two of the five subjects for which OCT data were available (Table 2). When this analysis was performed separately for 260- and 520-μm electrodes, a similar negative correlation was found between impedance and distance of the electrode from the retinal surface for both sizes of electrodes. For 260-μm electrodes, there was a significant negative correlation in two of the four subjects. One subject (S4) showed a positive correlation between electrode–retina distance and impedance. For 520-μm electrodes there was a significant negative correlation in two of the four subjects.

As shown in Figure 7d, there was no correlation between electrode distance and retinal thickness ($P > 0.05$). S5 showed a positive correlation between electrode distance from the retinal surface and retinal thickness, which may have been due to a slight compression of the retinal surface by the array in this subject.

As shown in Figure 7e, across subjects, there was no correlation between retinal thickness and threshold ($P > 0.05$). Within the five individual subjects, one (S6) had a slight positive correlation and another (S2) showed a slight negative correlation.

As shown in Figure 7f, across subjects there was no correlation between retinal thickness and impedance ($P > 0.05$). Two subjects (S3, S6) showed significant negative correlations, and one (S4, shown in italics) showed a significant positive correlation. When this analysis was performed separately for 260- and 520-μm electrodes, a negative correlation was found between retinal thickness and impedance for 260-μm electrodes. For 260-μm electrodes, there was a significant negative correlation in three of the four subjects, whereas the fourth (S4) showed a positive correlation between retinal thickness and impedance. For 520-μm electrodes

one subject (S6) showed a negative correlation between retinal thickness and impedance, and another (S4) showed a positive correlation.

Discussion

Threshold Sensitivity

As shown in Figure 3, the thresholds of our more sensitive subjects were significantly lower than have been reported, both for data reported earlier for S1–S3[9,15,30] and for earlier acute studies.[37] In our subjects who underwent later implantation, electrical stimulation thresholds are comparable to those reported in the animal literature (which to date has focused on the nondegenerated retina). This finding is surprising, given that the definition of threshold routinely used within in vitro studies of electrical stimulation is the current that reliably elicits at least one spike in a single cell. However, it has been shown that subjects with normal vision can reliably detect a single photon of light,[38] suggesting that a very small increase over the baseline firing rate of ganglion cells is probably sufficient to mediate behavioral detection. These data suggest that the sensitivity of degenerated human retina to electrical stimulation may not be greatly worse than the sensitivity of nondegenerated mammalian retina, as measured in vitro.

No Evidence of Tissue Damage

It is likely that retinal degeneration continued in our subjects as part of the natural progression of their disease. It was also a possibility that long-term stimulation may have led to retinal tissue damage. We did not see any systematic changes in retinal thickness over time; however, retinal changes may have occurred that did not affect retinal thickness, or that resulted in retinal thickness changes that were too subtle for us to observe.

However, it is worth noting that we did not see any gradual increases in threshold or impedance that were not associated with shifts in the distance of the electrode array from the retinal surface. In subjects S4 and S6, OCT measurements were taken over an extended period, during which the electrode array remained stable. During this period, changes in threshold and impedance tended to be relatively small (Fig. 5, S6). Thus, any postoperative changes in the retinal surface that may have occurred during these experiments did not have a measurable effect on retinal thickness, sensitivity, or impedance.

No Evidence of Electrode Corrosion

It was also possible that long-term stimulation led to electrode corrosion. It should be noted that any corrosion was unlikely to affect the measured distance of the electrode array from the retinal surface, because these measurements were taken from the top of the electrode. However, severe corrosion would have been likely to result in gradual increases in thresholds and impedance. As described earlier, we did not see large changes in threshold or impedance that were unassociated with shifts in the position of the array. Thus, any postoperative changes in the electrodes' surface that occurred did not have a measurable effect on either sensitivity or impedance.

Thresholds as a Function of Electrode Size

As described in Figures 3 and 4, we found that thresholds were the same for 260- and 520-μm electrodes. This is in contradiction to a recent literature review by Sekirnjak et al.,[17] who found, across a wide range of in vitro and in vivo studies, that log thresholds increase linearly with log electrode area, with a slope of 0.7. However, as shown in Figure 4b, it is possible that a wider range of electrode sizes would make threshold differences as a function of electrode size more apparent. Given the large electrode sizes used in this experiment, it is likely that

current density concentrated in a “ring” around the electrode edges.[39–42] As a result, for relatively large electrodes, the peak charge density for a given charge would differ less as a function of electrode size than would be predicted from their relative surface areas. Smaller electrodes would be expected to have more even current distribution across the electrode surface.

In this study, we measured perceptual threshold, which is the current needed for stimulation to be detected reliably. Useful prosthetic vision will, of course, require suprathreshold stimulation. Nonetheless, thresholds provide an indication of the lower limit beyond which it will be difficult to reduce electrode size. The low stimulation levels needed to detect phosphenes in two of our subjects imply that the suprathreshold stimulation levels required for useful prosthetic vision are likely to be attainable with smaller electrode sizes than those used in this study, provided the array is close to the retinal surface. The results from both S5 and S6 show thresholds consistently below 100 μA (0.975 ms pulse) on a majority of the electrodes. If it is assumed that platinum has a conservative, safe, long-term stimulation limit of 0.35 mC/cm^2,[34,35] then these data imply that electrodes of less than 200 μm in diameter would be acceptable. More advanced materials such as iridium oxide, with a safe stimulation limit of 3 mC/cm^2,[43] could safely permit the use of electrodes of 65 μm diameter. Reducing electrode size will permit more electrodes within the same retinal area, translating into more pixels per degree of visual angle. Simulations of prosthetic vision suggest that more electrodes in the central visual area of the retina may lead to a higher-resolution image and better visual task performance.[44,45]

The Relationship between Electrode Distance from the Retinal Surface, Impedance, and Threshold

Our data suggest that distance from the retinal surface is a critical factor in determining both threshold and impedance. For a given electrode size, electrodes that are close to the retinal surface have lower thresholds and higher impedances. As shown in Figure 7b, we see a positive correlation between threshold current and electrode distance from the retina. These data confirm retinal electrophysiology data, suggesting that the distance of the electrodes from the retina is a significant concern.[36,46] Stimulus current requirements are likely to be minimized when the array is in close position to the retina, minimizing power consumption by the stimulator, and allowing for smaller electrodes to generate phosphenes within safe charge density limits.

As would be expected, impedances are lower for larger electrodes. However, impedances are also negatively correlated with the distance of the electrode from the retinal surface (Fig. 7c). These data are consistent with the notion that electrodes that are close to the surface of the retina have higher impedances (because of the adjacent retinal tissue) than electrodes that have lifted from the retina (where fluid with higher conductivity intervenes between the electrode and the retinal surface).[36,47]

The electrode arrays used in this study were handmade and were relatively large and stiff. Consequently, a possible explanation for the changes in impedance and threshold that we see is that the single tack that was used to fix the array onto the retina permitted small amounts of array movement. It is plausible that the distance of electrodes from the retinal surface is the common factor responsible for the negative correlation between threshold and impedance. The relationship between electrode distance from the retinal surface, impedance, and threshold can been seen very clearly in S2 (Fig. 5). A lifting of the array (observed using fundus imaging since OCT imaging was not available at the time) led to an increase in thresholds and a decrease in impedances. After the electrode array was reattached, the impedances increased and thresholds dropped. There was then a second gradual lifting of the electrode array from the

retinal surface, which was again accompanied by an increase in thresholds and a decrease in impedance.

Negative correlations between threshold and impedance were significant in five of the six subjects, suggesting that within individual subjects, impedance may be used to predict threshold for a given electrode size. This method may prove useful for arrays with very high electrode counts, where measuring individual thresholds for each electrode would be impracticably time consuming.

As more advanced OCT imaging techniques become available,[48–50] it may be feasible, in the next generation of retinal implants, to track short-term changes in the electrode to retina distance in the immediate postoperative period. Detailed information about the distance of the electrodes from the retinal surface will allow a much finer characterization of the relationship between threshold, impedance, and electrode position.

Conclusions

Our data suggest that maintaining close proximity between the electrode array and the retinal surface is likely to be critical in developing a successful retinal implant. As well as affecting threshold, it is also likely that the ability to produce small localized percepts will be compromised if the array is not close to the retinal surface. If this is the case, as thinner electrode structures are developed and maintaining stable attachment to the retina becomes more tractable,[51,52] we might expect impedance and threshold values to become more stable over time. With the use of electrode arrays that are stable and flush on the retinal surface, and more complex measures of perceptual performance than our simple threshold measure, it is likely that the influence of other factors such as electrode size, progression of retinal degeneration, and subject age will become more apparent.

Acknowledgments

The authors thank Anne-Marie Ripley and Grant Palmer for support on regulatory issues and comments on the manuscript.

Supported by Second Sight Medical Products, Inc., the Fletcher Jones Foundation, the National Institute of Health (EY012893), and Research to Prevent Blindness.

References

1. Sharma RK, Ehinger B. Management of hereditary retinal degenerations: present status and future directions. Surv Ophthalmol 1999;43(5):427–444. [PubMed: 10340561]
2. Heckenlively, JR.; Boughman, J.; Friedman, L. Retinitis Pigmentosa. Lippincott; Philadelphia: 1988. Diagnosis and classification of retinitis pigmentosa.; p. 21
3. Margalit E, Sadda SR. Retinal and optic nerve diseases. Artif Organs 2003;27(11):963–974. [PubMed: 14616515]
4. Loewenstein JI, Montezuma SR, Rizzo JF 3rd. Outer retinal degeneration: an electronic retinal prosthesis as a treatment strategy. Arch Ophthalmol 2004;122(4):587–596. [PubMed: 15078678]
5. Rizzo JF III, Wyatt J, Loewenstein J, Kelly S, Shire D. Perceptual efficacy of electrical stimulation of human retina with a microelectrode array during short-term surgical trials. Invest Ophthalmol Vis Sci 2003;44(12):5362–5369. [PubMed: 14638739]
6. Terasawa Y, Tashiro H, Uehara A, et al. The development of a multichannel electrode array for retinal prostheses. J Artif Organs 2006;9(4):263–266. [PubMed: 17171406]
7. Yanai D, Weiland JD, Mahadevappa M, Greenberg RJ, Fine I, Humayun MS. Visual performance using a retinal prosthesis in three subjects with retinitis pigmentosa. Am J Ophthalmol 2007;143:820–827. [PubMed: 17362868]

8. Zrenner E. Will retinal implants restore vision? Science 2002;295(5557):1022–1025. [PubMed: 11834821]

9. Humayun MS, de Juan E Jr, Weiland JD, et al. Pattern electrical stimulation of the human retina. Vision Res 1999;39(15):2569–2576. [PubMed: 10396625]

10. Rizzo JF III, Wyatt J, Loewenstein J, Kelly S, Shire D. Methods and perceptual thresholds for short-term electrical stimulation of human retina with microelectrode arrays. Invest Ophthalmol Vis Sci 2003;44(12):5355–5361. [PubMed: 14638738]

11. Humayun MS, Prince M, de Juan E Jr, et al. Morphometric analysis of the extramacular retina from postmortem eyes with retinitis pigmentosa. Invest Ophthalmol Vis Sci 1999;40(1):143–148. [PubMed: 9888437]

12. Marc RE, Jones BW. Retinal remodeling in inherited photoreceptor degenerations. Mol Neurobiol 2003;28(2):139–147. [PubMed: 14576452]

13. Marc RE, Jones BW, Watt CB, Strettoi E. Neural remodeling in retinal degeneration. Prog Retin Eye Res 2003;22(5):607–655. [PubMed: 12892644]

14. Santos A, Humayun MS, de Juan E Jr, et al. Preservation of the inner retina in retinitis pigmentosa: a morphometric analysis. Arch Ophthalmol 1997;115(4):511–515. [PubMed: 9109761]

15. Mahadevappa M, Weiland JD, Yanai D, Fine I, Greenberg RJ, Humayun MS. Perceptual thresholds and electrode impedance in three retinal prosthesis subjects. IEEE Trans Neural Syst Rehabil Eng 2005;13(2):201–206. [PubMed: 16003900]

16. Jensen RJ, Ziv OR, Rizzo JF 3rd. Thresholds for activation of rabbit retinal ganglion cells with relatively large, extracellular microelectrodes. Invest Ophthalmol Vis Sci 2005;46(4):1486–1496. [PubMed: 15790920]

17. Sekirnjak C, Hottowy P, Sher A, Dabrowski W, Litke AM, Chichilnisky EJ. Electrical stimulation of mammalian retinal ganglion cells with multielectrode arrays. J Neurophysiol 2006;95(6):3311–3327. [PubMed: 16436479]

18. Jensen RJ, Rizzo JF III, Ziv OR, Grumet A, Wyatt J. Thresholds for activation of rabbit retinal ganglion cells with an ultrafine, extracellular microelectrode. Invest Ophthalmol Vis Sci 2003;44(8):3533–3543. [PubMed: 12882804]

19. Palanker D, Vankov A, Huie P, Baccus S. Design of a high-resolution optoelectronic retinal prosthesis. J Neural Eng 2005;2(1):S105–S120. [PubMed: 15876646]

20. Loudin JD, Simanovskii DM, Vijayraghavan K, et al. Optoelectronic retinal prosthesis: system design and performance. J Neural Eng 2007;4(1):S72–S84. [PubMed: 17325419]

21. Walia S, Fishman G, Edward DP, Lindeman M. Retinal nerve fiber layer defects in RP patients. Invest Ophthalmol Vis Sci 2007;48(10):4748–4752. [PubMed: 17898300]

22. Jones BW, Watt CB, Frederick JM, et al. Retinal remodeling triggered by photoreceptor degenerations. J Comp Neurol 2003;464(1):1–16. [PubMed: 12866125]

23. Duan YY, Clark GM, Cowan RS. A study of intra-cochlear electrodes and tissue interface by electrochemical impedance methods in vivo. Biomaterials 2004;25(17):3813–3828. [PubMed: 15020157]

24. Dorman MF, Smith LM, Dankowski K, McCandless G, Parkin JL. Long-term measures of electrode impedance and auditory thresholds for the Ineraid cochlear implant. J Speech Hear Res 1992;35(5):1126–1130. [PubMed: 1447922]

25. Hughes ML, Vander Werff KR, Brown CJ, et al. A longitudinal study of electrode impedance, the electrically evoked compound action potential, and behavioral measures in nucleus 24 cochlear implant users. Ear Hear 2001;22(6):471–486. [PubMed: 11770670]

26. Henkin Y, Kaplan-Neeman R, Muchnik C, Kronenberg J, Hildesheimer M. Changes over time in electrical stimulation levels and electrode impedance values in children using the Nucleus 24M cochlear implant. Int J Pediatr Otorhinolaryngol 2003;67(8):873–880. [PubMed: 12880667]

27. Henkin Y, Kaplan-Neeman R, Muchnik C, Kronenberg J, Hildesheimer M. Changes over time in the psycho-electric parameters in children with cochlear implants. Int J Audiol 2003;42(5):274–278. [PubMed: 12916700]

28. Saunders E, Cohen L, Aschendorff A, et al. Threshold, comfortable level and impedance changes as a function of electrode-modiolar distance. Ear Hear 2002;23(suppl 1):28S–40S. [PubMed: 11883764]

29. Yanai D, Lakhanpal RR, Weiland JD, et al. The value of preoperative tests in the selection of blind patients for a permanent microelectronic implant. Trans Am Ophthalmol Soc 2003;101:223–228. [PubMed: 14971581]discussion 228−230
30. Humayun MS, Weiland JD, Fujii GY, et al. Visual perception in a blind subject with a chronic microelectronic retinal prosthesis. Vision Res 2003;43(24):2573–2581. [PubMed: 13129543]
31. Tucci, DL.; Niparko, JK. Medical and surgical aspects of cochlear implantation.. In: Niparko, JK.; Kirk, KI.; Mellon, NK.; Robbins, AM.; Tucci, DL.; Wilson, BS., editors. Cochlear Implants Principles Practices. Lippincott Williams & Wilkins; Philadelphia: 2000. p. 189-221.
32. Watson AB, Robson JG. Discrimination at threshold: labelled detectors in human vision. Vision Res 1981;21(7):1115–1122. [PubMed: 7314490]
33. Watson AB, Pelli DG. QUEST: a Bayesian adaptive psychometric method. Percept Psychophys 1983;33(2):113–120. [PubMed: 6844102]
34. Brummer SB, Robblee LS, Hambrecht FT. Criteria for selecting electrodes for electrical stimulation: theoretical and practical considerations. Ann NY Acad Sci 1983;405:159–171. [PubMed: 6575640]
35. Brummer SB, Turner MJ. Electrical stimulation with Pt electrodes: II-estimation of maximum surface redox (theoretical non-gassing) limits. IEEE Trans Biomed Eng 1977;4(5):440–443. [PubMed: 892838]
36. Shah S, Hines A, Zhou D, Greenberg RJ, Humayun MS, Weiland JD. Electrical properties of retinal-electrode interface. J Neural Eng 2007;4(1):S24–S29. [PubMed: 17325413]
37. Humayun MS, de Juan E Jr, Dagnelie G, Greenberg RJ, Propst RH, Phillips DH. Visual perception elicited by electrical stimulation of retina in blind humans. Arch Ophthalmol 1996;114(1):40–46. [PubMed: 8540849]
38. Hecht S, Shlaer S, Pirenne MH. Energy at the threshold of vision. Science 1942;93(2425):585–587. [PubMed: 17795956]
39. Rubinstein JT, Spelman FA, Soma M, Suesserman MF. Current density profiles of surface mounted and recessed electrodes for neural prostheses. IEEE Trans Biomed Eng 1987;34(11):864–875. [PubMed: 3319885]
40. Suesserman MF, Spelman FA, Rubinstein JT. In vitro measurement and characterization of current density profiles produced by nonrecessed, simple recessed, and radially varying recessed stimulating electrodes. IEEE Trans Biomed Eng 1991;38(5):401–408. [PubMed: 1874521]
41. Wiley JD, Webster JG. Analysis and control of the current distribution under circular dispersive electrodes. IEEE Trans Biomed Eng 1982;29(5):381–385. [PubMed: 7084970]
42. Wiley JD, Webster JG. Distributed equivalent-circuit models for circular dispersive electrodes. IEEE Trans Biomed Eng 1982;29(5):385–389. [PubMed: 7084971]
43. Beebe X, Rose TL. Charge injection limits of activated iridium oxide electrodes with 0.2 ms pulses in bicarbonate buffered saline. IEEE Trans Biomed Eng 1988;35(6):494–495. [PubMed: 3397105]
44. Hayes JS, Yin VT, Piyathaisere D, Weiland JD, Humayun MS, Dagnelie G. Visually guided performance of simple tasks using simulated prosthetic vision. Artif Organs 2003;27(11):1016–1028. [PubMed: 14616520]
45. Thompson RW, Barnett GD, Humayun MS, Dagnelie G. Facial recognition using simulated prosthetic vision. Invest Ophthalmol Visual Sci 2003;44:5035–5042. [PubMed: 14578432]
46. Hesse L, Schanze T, Wilms M, Eger M. Implantation of retina stimulation electrodes and recording of electrical stimulation responses in the visual cortex of the cat. Graefes Arch Clin Exp Ophthalmol 2000;238(10):840–845. [PubMed: 11127571]
47. Heynen H, van Norren D. Origin of the electroretinogram in the intact macaque eye. II. Current source-density analysis. Vision Res 1985;25(5):709–715. [PubMed: 4024471]
48. Costa RA, Skaf M, Melo LA Jr, et al. Retinal assessment using optical coherence tomography. Prog Retin Eye Res 2006;25(3):325–353. [PubMed: 16716639]
49. Srinivasan VJ, Wojtkowski M, Fujimoto JG, Duker JS. In vivo measurement of retinal physiology with high-speed ultrahigh-resolution optical coherence tomography. Opt Lett 2006;31(15):2308–2310. [PubMed: 16832468]
50. Wojtkowski M, Srinivasan V, Fujimoto JG, et al. Three-dimensional retinal imaging with high-speed ultrahigh-resolution optical coherence tomography. Ophthalmology 2005;112(10):1734–1746. [PubMed: 16140383]

51. Guven D, Weiland JD, Maghribi M, et al. Implantation of an inactive epiretinal poly(dimethyl siloxane) electrode array in dogs. Exp Eye Res 2006;82(1):81–90. [PubMed: 16125701]

52. Walter P, Szurman P, Vobig M, et al. Successful long-term implantation of electrically inactive epiretinal microelectrode arrays in rabbits. Retina 1999;19(6):546–552. [PubMed: 10606457]

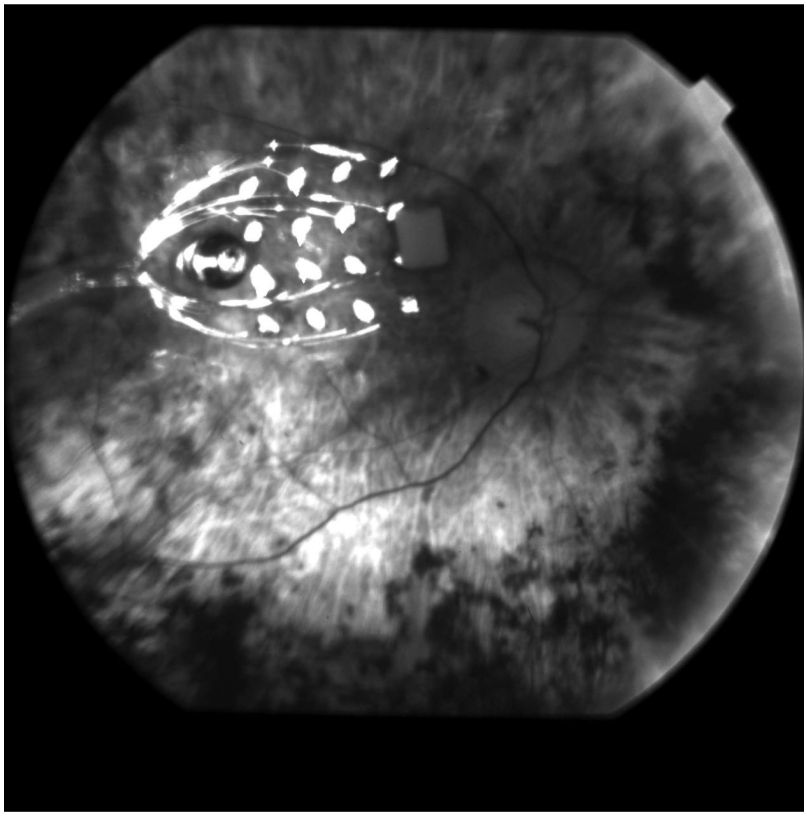

Figure 1.
Fundus photograph of an intraocular stimulating array viewed through a dilated pupil.

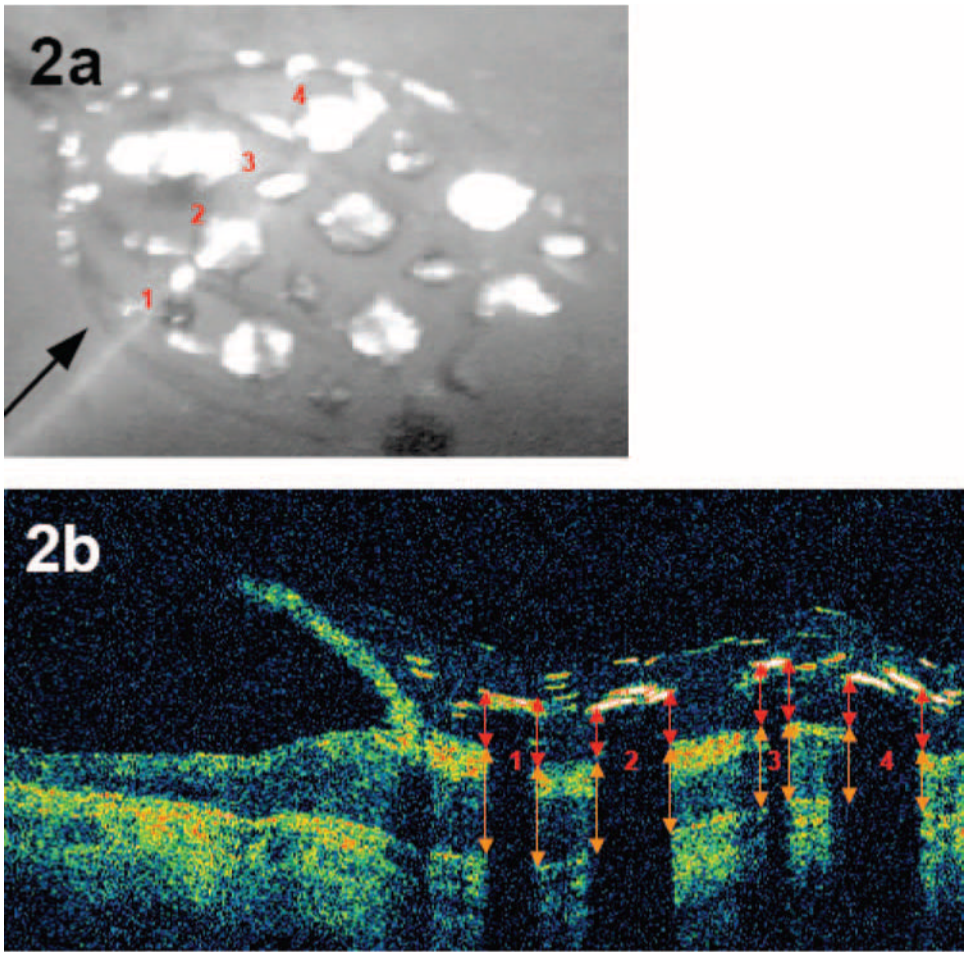

Figure 2.
OCT imaging of the array. (**a**) Fundus photograph of an intraocular electrode array viewed through a dilated pupil, imaged by the OCT system, just previous to the cross-sectional OCT image shown in (**b**). (**b**) Cross-sectional OCT image, in which the color represents log reflection. *Red* and *orange arrows* indicate how electrode distance and retinal thickness were measured.

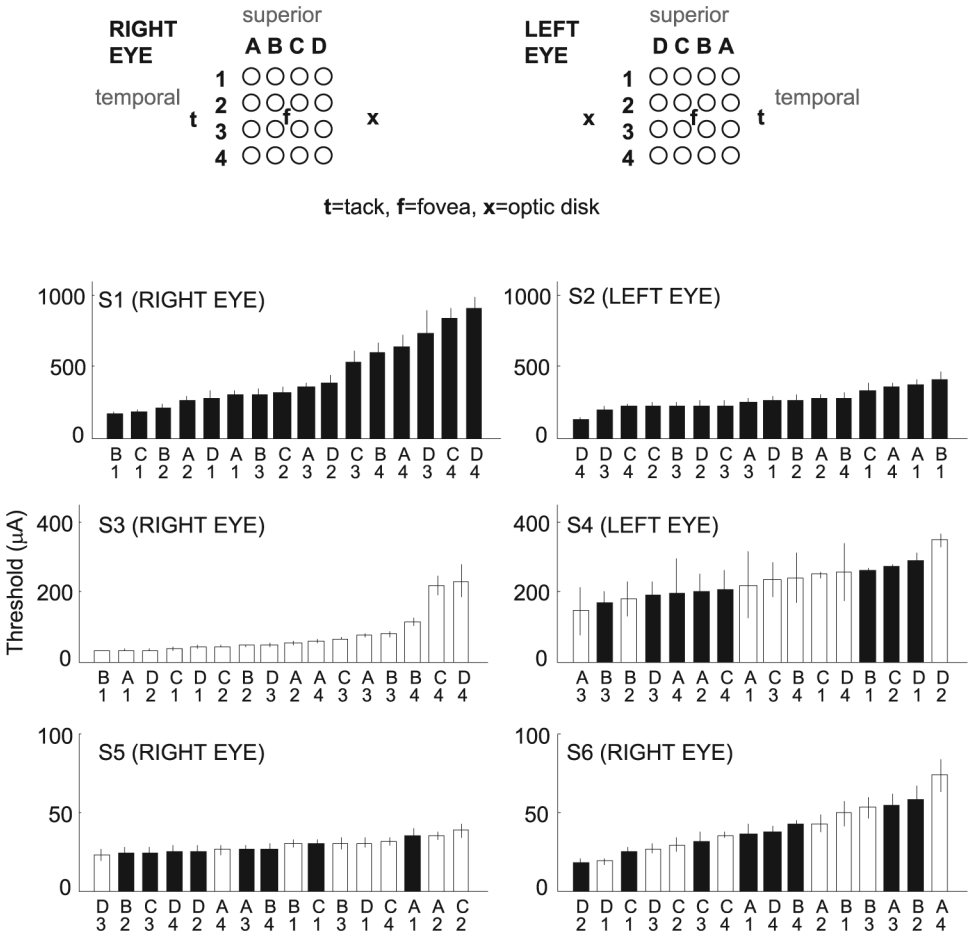

Figure 3.

Mean thresholds across the entire period of implantation of all 16 electrodes in each subject. *Top*: labeling scheme used to identify electrodes, as viewed through the pupil. In each subject, electrodes were ordered from most to least sensitive along the *x*-axis. Electrode diameters were (□) 260 and (■) 520 μm, respectively. Threshold current is shown along the *y*-axis. Note the dramatic change of scale along the *y*-axis across subjects. Error bars, ±1 SEM.

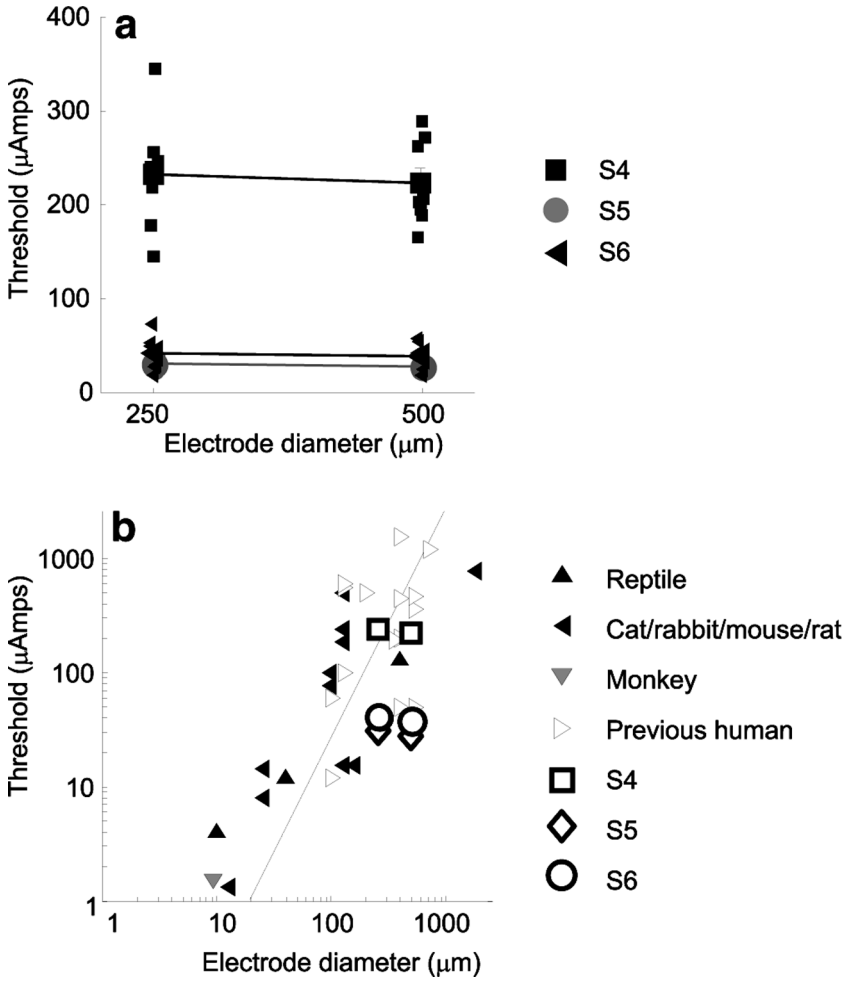

Figure 4.

Thresholds as a function of electrode diameter. (**a**) The *x*-axis represents electrode diameter and the *y*-axis represents the electrical stimulation threshold. Data from electrodes in subjects S4 to S6, implanted in a checkerboard configuration, are shown. *Symbols connected by lines*: mean threshold across each of the eight electrodes of a given diameter in each subject. Error bars, ±1 SEM. In many cases, error bars are smaller than the symbols. Individual electrodes are shown with small symbols. (**b**) Comparison of our thresholds to those reported in the literature. Replotted from Sekirnjak et al.[17] *Dashed line*: charge density limits of 0.35 mC/cm^2.

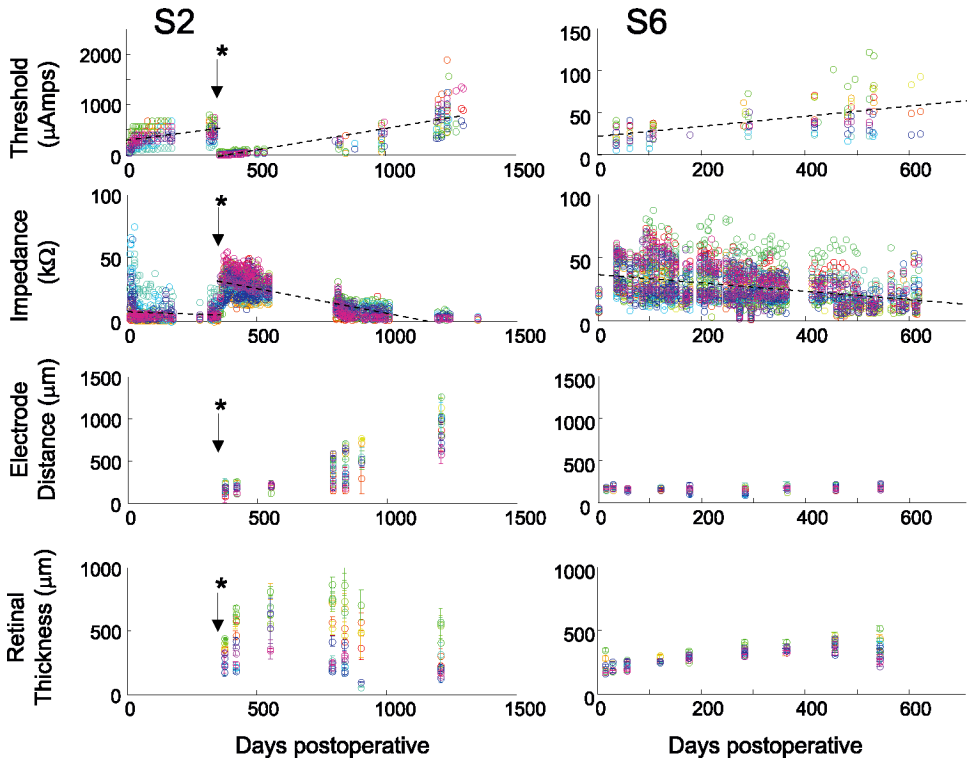

Figure 5.

Thresholds, impedance, distance between the electrodes and the retinal surface, and retinal thickness as a function of time in two subjects. Each color represents a different electrode. The *x*-axis represents days after surgery. In each subject, we calculated the best-fitting linear regression over time across all electrodes. *First row*: thresholds as a function of time. The *y*-axis represents threshold current for a 0.975-ms pulse. Note that both *x*- and *y*-axes differ across subjects. *S2's array detached from the retina after 11 months when the subject fell and bumped her head, and the array was then reattached. For this subject, we calculated separate linear regressions for each array attachment. Thresholds were lower and impedances higher after reattachment. For both subjects the mean best-fitting linear regression line (across all electrodes) is shown (*black dotted line*). *Second row*: impedance as a function of time. The mean best-fitting linear regression line (across all electrodes) is shown (*black dotted line*). *Third row*: distance between the electrodes and the retinal surface, as measured with OCT. *Fourth row*: retinal thickness as measured with OCT. Error bars, ± 1 SEM.

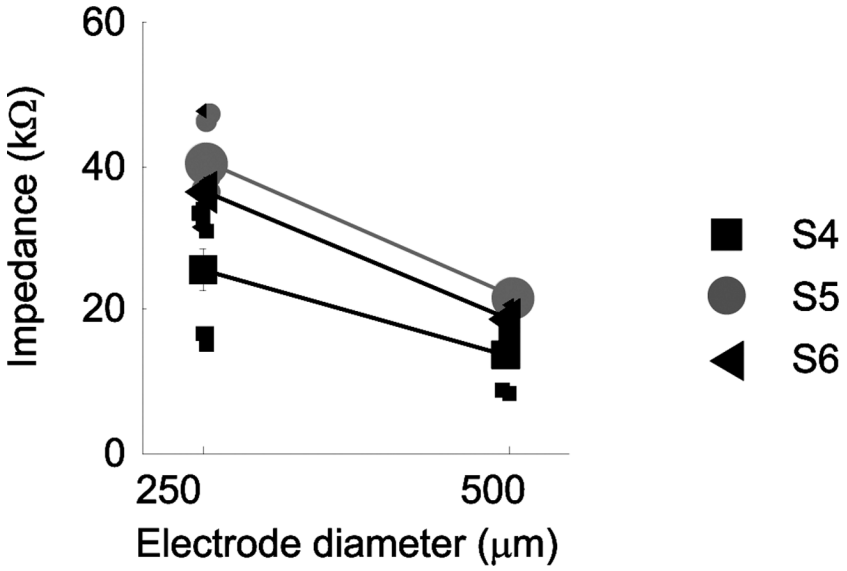

Figure 6.
Impedance as a function of electrode diameter. *Large symbols* connected by *lines*: mean impedance across each of the eight electrodes of a given diameter for each subject. *Small symbols*: individual electrodes. Error bars, ± 1SEM. In many cases, error bars are smaller than the symbols.

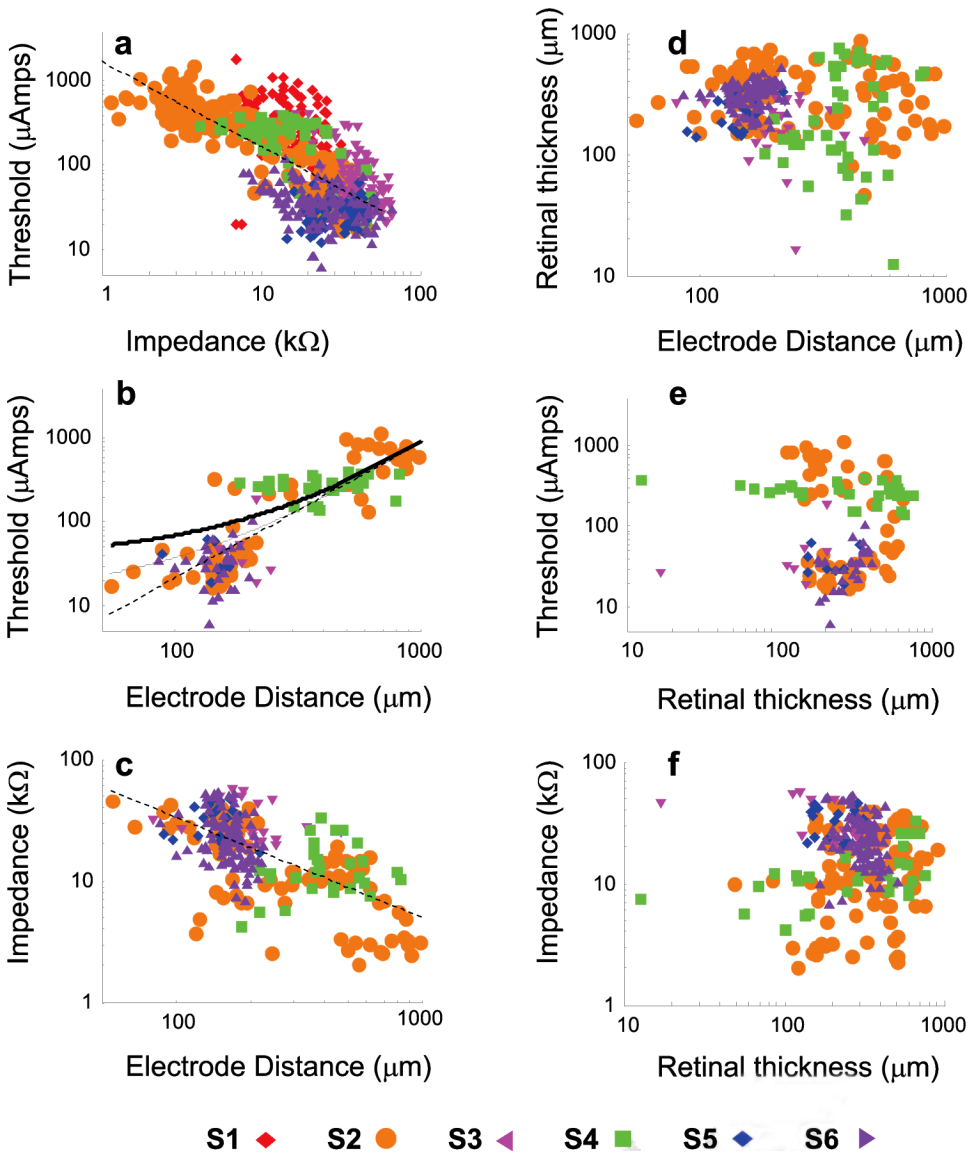

Figure 7.

Correlations between threshold, impedance, electrode distance, and retinal thickness on log–log axes. Each subject is shown with a different color and symbol shape. *Dashed lines*: best-fitting linear regression on log–log axes. (**a**) Impedance versus threshold. (**b**) Electrode distance from the retinal surface versus threshold. *Curved solid lines*: predicted thresholds for 260 (*bottom, thin solid line*) and 560 μm (*top, thick solid line*) electrodes based on the model of Palanker et al.[19] (**c**) Electrode distance from the retinal surface versus impedance. (**d**) Electrode distance versus retinal thickness. (**e**) Retinal thickness versus threshold. (**f**) Retinal thickness versus impedance.

Table 1

Details of Surgical Implantation and Measurement Data for Each Subject

Subject	Age at Implantation	Implanted Eye	Preoperative VA (Implanted)	Preoperative VA (Nonimplanted)	Data Range (days)	Electrode Size (μm)
S1	76	R	NLP	LP	1087	520
S2	56	L	LP	LP	1299	520
S3	74	R	NLP	NLP	833	260
S4	60	L	LP	LP	154	260/520
S5	59	R	LP	LP	656	260/520
S6	55	R	NLP	NLP	621	260/520

Acuities were based on the ability to detect a handheld light. When a Ganzfeld or photographic flash was used, all subjects were capable of seeing light. The eye requiring higher light levels to achieve perception was deemed less sensitive. VA, visual acuity; NLP, no light perception; LP, light perception.

Table 2

Statistical Results for Figure 7

Figure Panel	Electrodes	Across Subjects e	Across Subjects f	Across Subjects *P*	Subject	Within Subjects e	Within Subjects f	Within Subjects *P*
7a. Threshold vs. impedance	All	*−1.01*	*1808*	***	S1	*−14.1*	*585.6*	***
					S2	*−15.8*	*528.9*	***
					S3	*−4.4*	*258.5*	***
					S4	*−6.2*	*330.4*	***
					S6	*−0.58*	*53.7*	***
	260 µm	*−0.43*	*5.3*	***	S3	*−4.4*	*258.5*	***
					S4	*−13.5*	*369.7*	***
					S6	*−1.7*	*68.1*	***
	520 µm	*−1*	*7.6*	***	S1	*−14.1*	*585.6*	***
					S2	*−15.8*	*528.9*	***
					S4	*−8.2*	*411.9*	***
					S6	*−0.9*	*70.8*	***
7b. Threshold vs. electrode distance	All	0.23	3.8	***	S2	1.98	60.5	***
					S6	0.75	26.5	*P* = 0.05
7c. Impedance vs. electrode distance	All	*−0.08*	*3.1*	**	S2	*−0.08*	*24.5*	***
					S6	*−0.4*	*30.7*	***
	260 µm	*−0.04*	*2.9*	*	S4	*0.02*	*6.3*	*
					S5	*−0.1*	*23.3*	***
					S6	*−0.1*	*18.6*	*
	520 µm	*−0.1*	*3.2*	***	S2	*−0.08*	*24.5*	***
					S5	*−0.4*	*37.4*	*
7d. Retinal thickness vs. electrode distance	All			NS	S5	1.4	91.2	*
7e. Threshold vs. retinal thickness	All			NS	S2	*−1.49*	*460.2*	*
					S6	0.37	−12.2	***
7f. Impedance vs. retinal thickness	All			NS	S3	*−0.3*	*55*	**
					S4	0.04	7	**
					S6	*−0.1*	*40.9*	***
	260 µm	*−0.2*	*3.9*	*	S3	*−0.3*	*55*	***
					S4	0.02	6.4	*
					S5	*−0.06*	*27.6*	*
					S6	*−0.05*	*23.7*	*
	520 µm			NS	S4	0.06	7.55	***
					S6	*−0.11*	*46.3*	*

Individual subjects' (S) values for the exponent (e), multiplicative scaling factor (f), and fit significance (p) for the regression lines in Figures 7a-7f. NS, not significant. Negative correlations are shown in italics.

* $P < 0.05$.

** $P < 0.01$.

*** $P < 0.001$.